Bose-Einstein partition distribution in microcavity quantum superradiance

E. De Angelis,[1] F. De Martini,[2] P. Mataloni,[2] and M. Giangrasso[3]
[1]*Istituto di Fisica dello Spazio Interplanetario, CNR, Roma 00100, Italy*
[2]*Dipartimento di Fisica and Istituto Nazionale per la Fisica della Materia, Università di Roma "La Sapienza," Roma 00185, Italy*
[3]*Tecnomultimediale Produzione, Roma 00154, Italy*
(Received 12 September 2000; published 11 July 2001)

The paper reports the realization of the process of two-dipole Dicke superradiance in a planar optical microcavity. Two dye molecules, located at a mutual distance $|\mathbf{R}|$ within the transverse resonant mode of the microcavity, are excited by two independent femtosecond pulses. The superradiant photon emission by the two systems and the consequent enhancement of the time decay of the dipole excitation is investigated. Furthermore, the spatial counterpart of superradiance is revealed by the realization of the Bose-Einstein partition statistics within the detection of photons emitted over the two output sides of the microcavity. A general quantum analysis of the process is given in the paper.

DOI: 10.1103/PhysRevA.64.023809 PACS number(s): 42.50.Dv, 32.50.+d, 42.50.Vk

I. INTRODUCTION

The introduction of the concept of optical microscopic cavity (microcavity) has produced some relevant scientific advances, with implications on the technological and on the fundamental sides. We mention the possibility of modifying the atomic spontaneous emission (SE) [1,2], the transition spontaneous-stimulated emission in a thresholdless microlaser [3], and the introduction of the concept of *transverse coherence* length in a planar microcavity [4].

Recently we have demonstrated that a single-mode planar microcavity with relevant dimension $d=\lambda/2$ may behave as a reliable and efficient source of single-photon radiation, with a nonclassical sub-Poissonian distribution, if few fluorescent dye molecules trapped between the cavity mirrors are excited by femtosecond laser pulses [5]. Because of the ultrafast excitation each molecule can absorb a single pump photon only once during the pump pulse duration, without recycling between the lower and the excited level, and reemits a single photon at the wavelength λ over the only allowed mode of the microcavity.

The single-photon generation process can be doubled by exciting two dipoles, or two ensembles of dipoles, which are assumed to be at rest a distance $\mathbf{R}$ apart in the transverse plane of the microcavity. In these conditions, inter dipole coupling occurring between the two quantum objects via a superradiant-type process is expected [6,7].

The study of atomic superradiant interaction has represented an important topic of fundamental physics. If the two atoms are situated in free space at a mutual distance $R<\lambda$, the wavelength of atomic emission, the SE rate can be doubled with respect to the corresponding rate of a single atom [8]. This *temporal* aspect of the superradiance process was experimentally investigated by Gross and Haroche [9] and, more recently, by De Voe and Brewer [10]. In the case of two dipoles trapped within a planar high finesse microcavity the mutual interaction is established at a relative distance much larger than the wavelength of emission. Provided that $R=|\mathbf{R}|\leqslant l_c$, the transverse coherence length of the microcavity [4,11] or, equivalently, the effective mode radius of the electromagnetic (e.m.) field [12], the field involved in the inter-atomic coupling belongs to the common cavity spatial mode and the transverse interaction can be established with a retardation time, $\tau_r=R/c$, which is much shorter than the cavity photon lifetime, $\tau_c=f(\lambda/2\pi c)$. In the above expressions $l_c=2\lambda\sqrt{f}$, where $f=\pi|r|/(1-|r|^2)$ corresponds to the finesse of a cavity terminated by two equal mirrors, with complex reflection coefficients at normal incidence $r=r_1=r_2$. In the case of two highly reflecting multilayer dielectric mirrors, l_c can be as large as 100 μm, and interdipole interaction occurs in the subpicosecond time scale [13,14].

In a recent experiment [15] we have investigated the process of superradiant spontaneous emission from a two-dipole system confined in a planar microcavity. By this technique it was possible to verify the expected temporal behavior of superradiance. Furthermore, the investigation of this process in the space domain allowed us to discover an unexpected collective Bose-Einstein distribution of the photons emitted by the microcavity *as a whole*, over the modes $\mathbf{k}$ and $\mathbf{k}'$, corresponding to the two output sides of the microcavity.

In the present paper the full theory of the process of two-dipole superradiant emission within a planar microcavity is reported and discussed. Furthermore, we give a detailed description of the experiment of Ref. [15], and of the relative experimental results.

The work is organized as follows: in Sec. II, after the introduction of the radiation field quantization and of the interaction Hamiltonian, we discuss the process of two-dipole correlation within a microcavity. The expression of the rate of two-dipole superradiant spontaneous emission is given in Sec. III, where the second-order correlation function of the field radiated by the two-dipole system is also defined. The description of the experiment and the experimental results are given in Sec. IV. Finally, an extended discussion of the results is reported in Sec. V.

II. TWO-DIPOLE CORRELATION WITHIN THE MICROCAVITY

The theoretical analysis of the process of two-dipole correlation via transverse interaction in a microcavity can start by expressing the e.m. field in terms of the cavity mode

functions $U_{\mathbf{k}j}(\mathbf{r})$ and $U'_{\mathbf{k}j}(\mathbf{r})$, previously introduced by Ley and Loudon [16]. We refer to their expression given in the extended theory of spontaneous emission in a Fabry-Pèrot microcavity [2]. The e.m. field is quantized by the introduction of mode creation and destruction operators. The operators for the modes with spatial functions $U_{\mathbf{k}j}(\mathbf{r})$ and $U'_{\mathbf{k}j}(\mathbf{r})$ are denoted $\hat{a}^{\dagger}_{\mathbf{k}j}, \hat{a}_{\mathbf{k}j}$ and $\hat{a}'^{\dagger}_{\mathbf{k}j}, \hat{a}'_{\mathbf{k}j}$, respectively. The wave vector $\mathbf{k}$ is assumed to be a continuous variable, a function of the polar angles ϑ and φ [2]. For each set of polar angles there are two transverse polarization directions with indexes $j=1, 2$ associated with unit vectors $\boldsymbol{\varepsilon}(\mathbf{k},j)$ [2]. The field operators satisfy the commutations relations,

$$[\hat{a}_{\mathbf{k}j}, \hat{a}^{\dagger}_{\mathbf{k}'j'}] = [\hat{a}'_{\mathbf{k}j}, \hat{a}'^{\dagger}_{\mathbf{k}'j'}] = \delta_{jj'}\delta(\mathbf{k}-\mathbf{k}'), \tag{1}$$

$$[\hat{a}_{\mathbf{k}j}, \hat{a}'^{\dagger}_{\mathbf{k}'j'}] = [\hat{a}'_{\mathbf{k}j}, \hat{a}^{\dagger}_{\mathbf{k}'j'}] = 0. \tag{2}$$

The mode operators allow one to define the normal-ordered part of the e.m. field Hamiltonian expressed in integral form,

$$\hat{H}_F = \int d\mathbf{k}\, \hbar c k \sum (\hat{a}^{\dagger}_{\mathbf{k}j}\hat{a}_{\mathbf{k}j} + \hat{a}'^{\dagger}_{\mathbf{k}j}\hat{a}'_{\mathbf{k}j}), \tag{3}$$

where the three-dimensional integral is expressed as

$$\int d\mathbf{k} = \int_0^{+\infty} dk \int_0^{\pi/2} d\vartheta \int_0^{2\pi} d\varphi\, k^2 \sin\vartheta. \tag{4}$$

The Hamiltonian of a two-level atomic system is defined as

$$\hat{H}_0 = \hbar\omega\, \hat{\pi}^{\dagger}\hat{\pi}, \tag{5}$$

with $\omega = 2\pi c/\lambda$. Here the transition atomic operators $\hat{\pi}^{\dagger} = |e\rangle\langle g|$ and $\hat{\pi} = |g\rangle\langle e|$ are associated with the ground and excited energy levels $|g\rangle$ and $|e\rangle$. The following properties are satisfied:

$$\begin{aligned} &\hat{\pi}^{\dagger}\hat{\pi}^{\dagger} = \hat{\pi}\hat{\pi} = 0, \\ &[\hat{\pi}, \hat{\pi}^{\dagger}] = 1 - 2\hat{\pi}^{\dagger}\hat{\pi} = 2\hat{\pi}\hat{\pi}^{\dagger} - 1. \end{aligned} \tag{6}$$

The expressions $\hat{\pi}\hat{\pi}^{\dagger} = |g\rangle\langle g|$ and $\hat{\pi}^{\dagger}\hat{\pi} = |e\rangle\langle e|$ correspond to the populations of the levels $|g\rangle$ and $|e\rangle$ and satisfy the completeness relation for a two-level atom:

$$\hat{\pi}\hat{\pi}^{\dagger} + \hat{\pi}^{\dagger}\hat{\pi} = 1. \tag{7}$$

The interaction Hamiltonian is expressed in electric dipole approximation as a function of the electric-field operator $\hat{\mathbf{E}}(\mathbf{r},t)$ and the dipole operator $\hat{\mathbf{D}}, \hat{H}_I(\mathbf{r},t) = \hat{\mathbf{D}}\cdot\hat{\mathbf{E}}(\mathbf{r},t)$. The electric-field operator is conveniently separated into two parts, $\hat{\mathbf{E}}(\mathbf{r},t) = \hat{\mathbf{E}}^{+}(\mathbf{r},t) + \hat{\mathbf{E}}^{-}(\mathbf{r},t)$, where $\hat{\mathbf{E}}^{+}(\mathbf{r},t)$ and $\hat{\mathbf{E}}^{-}(\mathbf{r},t)$ are written in integral form and modulated by the mode functions

$$\begin{aligned} \hat{\mathbf{E}}^{+}(\mathbf{r},t) = i\int d\mathbf{k} \sum_j \left(\frac{\hbar c k}{16\pi^3\varepsilon_0}\right)^{1/2} \boldsymbol{\varepsilon}(\mathbf{k},j)[U_{\mathbf{k}j}(\mathbf{r})\hat{a}_{\mathbf{k}j} \\ + U'_{\mathbf{k}j}(\mathbf{r})\hat{a}_{\mathbf{k}j}]e^{-ickt}, \end{aligned} \tag{8}$$

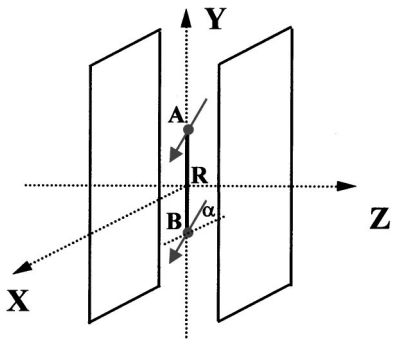

FIG. 1. Schematic of the planar microcavity with the dipoles A and B located at a mutual distance $\mathbf{R}$ on the symmetry plane $\mathbf{Z}=\mathbf{0}$.

$$\begin{aligned} \hat{\mathbf{E}}^{-}(\mathbf{r},t) = -i\int d\mathbf{k} \sum_j \left(\frac{\hbar c k}{16\pi^3\varepsilon_0}\right)^{1/2} \boldsymbol{\varepsilon}(\mathbf{k},j)[U^{*}_{\mathbf{k}j}(\mathbf{r})\hat{a}^{\dagger}_{\mathbf{k}j} \\ + U'^{*}_{\mathbf{k}j}(\mathbf{r})\hat{a}^{\dagger}_{\mathbf{k}j}]e^{ickt}. \end{aligned} \tag{9}$$

The dipole operator is expressed as

$$\hat{\mathbf{D}} = |e\rangle\langle e|\hat{\mathbf{D}}|g\rangle\langle g| + |g\rangle\langle g|\hat{\mathbf{D}}|e\rangle\langle e| = \mu[\hat{\pi} + \hat{\pi}^{\dagger}], \tag{10}$$

where $\mu = \langle e|\hat{\mathbf{D}}|g\rangle = \mathbf{D}_{eg}$ corresponds to the matrix element of the dipole operator. The expression of the interaction Hamiltonian obtained in the case of electric dipole approximation is

$$\begin{aligned} \hat{H}_I = i\int d\mathbf{k} \sum_j \left(\frac{\hbar c k}{16\pi\varepsilon_0}\right)^{1/2} \boldsymbol{\varepsilon}(\mathbf{k},j)\cdot\boldsymbol{\mu}[\hat{\pi}^{\dagger} + \hat{\pi}] \\ \times[U_{\mathbf{k}j}(\mathbf{r})\hat{a}_{\mathbf{k}j}e^{-ickt} - U^{*}_{\mathbf{k}j}(\mathbf{r})\hat{a}^{\dagger}_{\mathbf{k}j}e^{ickt} + U'_{\mathbf{k}j}(\mathbf{r})\hat{a}'_{\mathbf{k}j}e^{-ickt} \\ - U'^{*}_{\mathbf{k}j}(\mathbf{r})\hat{a}'^{\dagger}_{\mathbf{k}j}e^{ickt}]. \end{aligned} \tag{11}$$

We start to investigate the physical condition of two dipoles **A** and **B**, located on the symmetry plane $\mathbf{Z}=\mathbf{0}$ of a planar microcavity, interacting at a mutual transverse distance $\mathbf{R}$ along the **Y** direction (see Fig. 1). Their common dipole vectors $\boldsymbol{\mu}_A$ and $\boldsymbol{\mu}_B$, with $|\mu_A| = |\mu_B| = |\mu|$, are parallel to the mirror planes and oriented at an angle α with respect to the **X** axis.

The interaction Hamiltonian in Eq. (11) can now be reexpressed in the forms

$$\begin{aligned} \hat{H}_I = i\int d\mathbf{k} \sum_j g_j(\cos\vartheta) e^{i\mathbf{k}\cdot\mathbf{r}_A}\hat{c}_{kj}[\hat{\pi}^{\dagger}_A + \hat{\pi}_A + e^{i\mathbf{k}\cdot\mathbf{R}}(\hat{\pi}^{\dagger}_B \\ + \hat{\pi}_B)] + \text{H.c.}, \end{aligned} \tag{12}$$

where the function

$$g_j(\cos\vartheta) = \left(\frac{\hbar c k}{16\pi\varepsilon_0}\right)^{1/2} i|t|\,\frac{1-|r|e^{ikdc}}{\Delta}\,\boldsymbol{\varepsilon}(\mathbf{k},j)\cdot\boldsymbol{\mu} \tag{13}$$

accounts for the cavity confinement. In the last expression we have $\Delta = 1 - |r|^2 e^{2ikdc}$, and the confined electromagnetic field has been expressed in a simple fashion by the following

"quasimode" substitutions: $\hat{c}_{kj}=\hat{a}_{\mathbf{k}j}+\hat{a}'_{\mathbf{k}j}$ and $\hat{c}^{\dagger}_{kj}=\hat{a}^{\dagger}_{\mathbf{k}j}+\hat{a}'^{\dagger}_{\mathbf{k}j}$. These new operators satisfy the commutation relations $[\hat{c}_{kj},\hat{c}^{\dagger}_{kj}]=2\delta_{jj'}\delta(\mathbf{k}-\mathbf{k}')$.

The total Hamiltonian of the system becomes

$$\begin{aligned}\hat{H}_{\rm tot}&=\hat{H}_0+\hat{H}_F+\hat{H}_I\\&=\hbar\omega_0(\hat{\pi}^{\dagger}_A\hat{\pi}_A+\hat{\pi}^{\dagger}_B\hat{\pi}_B)+\int d\mathbf{k}\,\hbar ck\sum_j\\&\times(\hat{a}^{\dagger}_{\mathbf{k}j}\hat{a}_{\mathbf{k}j}+\hat{a}'^{\dagger}_{\mathbf{k}j}\hat{a}'_{\mathbf{k}j})+i\int d\mathbf{k}\sum_j g_j(\cos\vartheta)\\&\times e^{i\mathbf{k}\cdot\mathbf{r}_A}\hat{c}_{kj}[\hat{\pi}^{\dagger}_A+\hat{\pi}_A+e^{i\mathbf{k}\cdot\mathbf{R}}(\hat{\pi}^{\dagger}_B+\hat{\pi}_B)]+\text{H.c.}\end{aligned}\tag{14}$$

We may now investigate the time behavior of the upper level of dipole A under the influence of dipole B in the Heisenberg representation

$$\frac{d\hat{\pi}^{\dagger}_A\hat{\pi}_A}{dt}=-\frac{i}{\hbar}[\hat{\pi}^{\dagger}_A\hat{\pi}_A,\hat{H}_{\rm tot}].$$

By following a second-order perturbative approximation [7,17] we obtain

$$\begin{aligned}\frac{d\langle\hat{\pi}^{\dagger}_A\hat{\pi}_A\rangle_t}{dt}&=-2\Gamma\Bigg\{\langle\hat{\pi}^{\dagger}_A\hat{\pi}_A\rangle_0+\frac{3\hat{\mu}_i\hat{\mu}_h}{2k_0^3}\langle\hat{\pi}^{\dagger}_A\hat{\pi}_B\rangle_0C^R_{ih}\\&\times[\sin(k_0R)]\theta(ct-R)+\frac{3\hat{\mu}_i\hat{\mu}_h}{k_0^3}\sum_{n=1}^{+\infty}\\&(-|r|)^n\{\langle\hat{\pi}^{\dagger}_A\hat{\pi}_A\rangle_0C^{nd}_{ih}[\sin(k_0nd)]\theta(ct-nd)\\&+\langle\hat{\pi}^{\dagger}_A\hat{\pi}_B\rangle_0C^{R_n}_{ih}[\sin(k_0R_n)]\theta(ct-R_n)\}\Bigg\},\end{aligned}\tag{15}$$

where the indexes $i,h=1,2,3$ represent the spatial vector and tensor components. Here $\Gamma=1/2\tau_{\rm rad}=|\mu|^2k_0^3/6\pi\varepsilon_0\hbar$ corresponds to the characteristic free-space atomic spontaneous emission rate, $\theta(ct-x)$ are Heaviside unit step functions, and the general expression holds,

$$\begin{aligned}C^x_{ih}[\sin(k_0x)]&=k_0^3\Bigg\{(\delta_{ih}-\hat{x}_i\hat{x}_h)+\frac{\sin(k_0x)}{k_0x}+(\delta_{ih}-3\hat{x}_i\hat{x}_h)\\&\times\left[\frac{\cos(k_0x)}{(k_0x)^2}-\frac{\sin(k_0x)}{(k_0x)^3}\right]\Bigg\}.\end{aligned}\tag{16}$$

Note in Eq. (16) the appearance of the self-interaction contribution to to the spontaneous emission of the atom A: this one is expressed by the first term at the right-hand side (rhs) of Eq. (16). The effect of the presence of dipole B takes place through two different channels, i.e., by a direct nonconfined vacuum-field correlation, expressed by the second term at the rhs, and by a *confined-vacuum* process with intensity proportional to $|r|$. This last contribution is expressed by the series

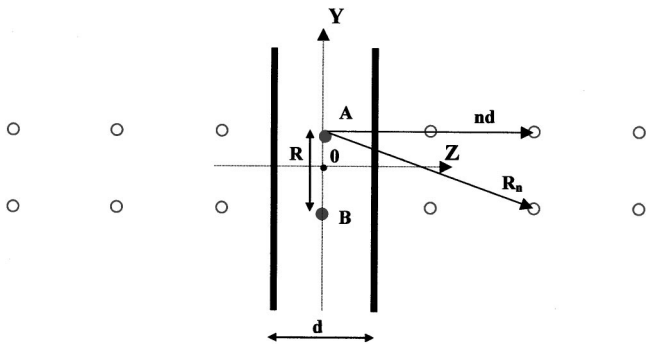

FIG. 2. Multiple images of the two-dipole system due to microcavity reflections.

with alternate signs appearing in the equation. The parameters nd and $R_n=\sqrt{R^2+(nd)^2}$ correspond precisely to the coordinates of the nth mirror images of dipole A and of dipole B, respectively [6,7] (cf. Fig. 2). As a consequence, the total decay rate, besides the free-space decay contribution, depends also on the coupling of each dipole with its own multiple images and with the multiple images of the other dipole.

For the sake of completeness, we give the explicit expression [7] of the SE rate of dipole A for two cases corresponding to different spatial orientations of the mutually parallel dipoles $\mu=\mu(\cos\alpha,\sin\alpha,0)$ with respect to the **X** axis (cf. Fig. 1).

Case 1. $\alpha=0$, dipoles parallel to the **X** axis,

$$\begin{aligned}\frac{d\langle\hat{\pi}^{\dagger}_A\hat{\pi}_A\rangle_t}{dt}&=-2\Gamma\Bigg(\langle\hat{\pi}^{\dagger}_A\hat{\pi}_A\rangle_0+\frac{3}{2k_0^3}\langle\hat{\pi}^{\dagger}_A\hat{\pi}_B\rangle_0\Bigg[\sin(k_0R)\\&\left(-\frac{1}{R^3}+\frac{k_0^2}{R}\right)+\cos(k_0R)\frac{k_0}{R^2}\Bigg]\theta(ct-R)\\&+\frac{3}{k_0^3}\sum_{n=1}^{+\infty}(-|r|)^n\Bigg\{\langle\hat{\pi}^{\dagger}_A\hat{\pi}_A\rangle_0\Bigg[\sin(k_0nd)\\&\left(-\frac{1}{n^3d^3}+\frac{k_0^2}{nd}\right)+\cos(k_0nd)\frac{k_0}{n^2d^2}\Bigg]\theta(ct-nd)\\&+\langle\hat{\pi}^{\dagger}_A\hat{\pi}_B\rangle_0\Bigg[\sin(k_0R_n)\left(-\frac{1}{R_n^3}+\frac{k_0^2}{R_n}\right)\\&+\cos(k_0R_n)\frac{k_0}{R_n^2}\Bigg]\theta(ct-R_n)\Bigg\}\Bigg).\end{aligned}\tag{17}$$

It is interesting to study the function which modulates the mutual terms,

$$\begin{aligned}D(t,R)&=\frac{3}{2k_0^3}\Bigg[\sin(k_0R)\left(-\frac{1}{R^3}+\frac{k_0^2}{R}\right)+\cos(k_0R)\frac{k_0}{R^2}\Bigg]\theta(ct\\&-R)+\frac{3}{k_0^3}\sum_{n=1}^{+\infty}(-|r|)^n\Bigg[\sin(k_0R_n)\left(-\frac{1}{R_n^3}+\frac{k_0^2}{R_n}\right)\\&+\cos(k_0R_n)\frac{k_0}{R_n^2}\Bigg]\theta(ct-R_n).\end{aligned}\tag{18}$$

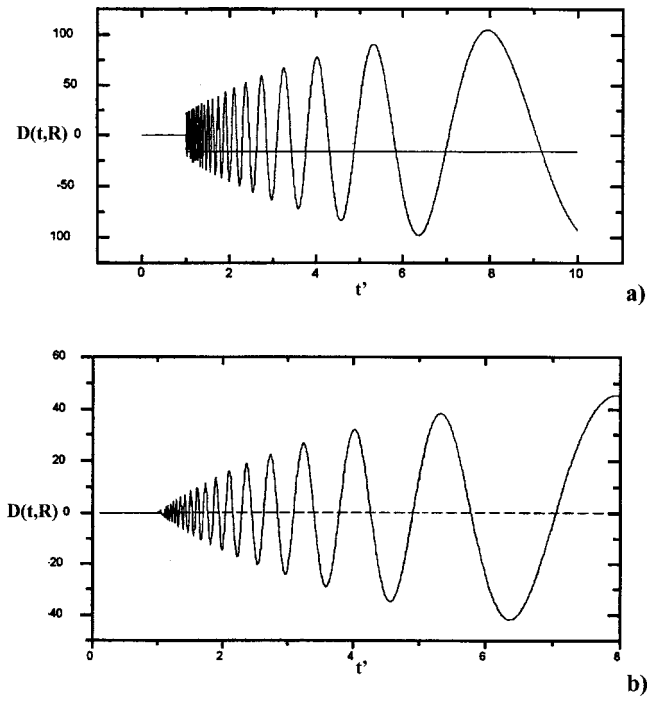

FIG. 3. Numerical evaluation of the mutual function $D(t,R)$ expressed by Eqs. (18) and (20). (a) Dipoles parallel to the **X** axis ($\alpha=0$). (b) Dipoles parallel to the **Y** axis ($\alpha=\pi/2$). It is calculated as a function of the normalized time $t'=ct/R$ for a relative interatomic distance $\gamma=R/l_c=0.5$, and for a microcavity finesse $f=1000$.

The interference with alternate signs affects the increasingly retarded interaction contribution to the spontaneous-emission rate of dipole *A*. This interference leads to the quasioscillatory result of Fig. 3(a), where the temporal behavior of $D(t,R)$ is shown. It is found to be largely dependent on the cavity finesse f and on the ratio $\beta=R/l_c$, expressing the degree of coexistence of the atoms within the same transverse cavity mode.

Case 2. $\alpha=\pi/2$, dipoles parallel to the **Y** axis,

$$\frac{d\langle\hat{\pi}_A^\dagger\hat{\pi}_A\rangle_t}{dt}=-2\Gamma\Bigg(\langle\hat{\pi}_A^\dagger\hat{\pi}_A\rangle_0+\frac{3}{2}\langle\hat{\pi}_A^\dagger\hat{\pi}_B\rangle_0\Bigg\{2\Bigg[-\frac{\cos(k_0R)}{k_0^2R^2}+\frac{\sin(k_0R)}{k_0^3R^3}\Bigg]\Bigg\}\theta(ct-R)+3\sum_{n=1}^{+\infty}(-|r|)^n\times\Bigg(\langle\hat{\pi}_A^\dagger\hat{\pi}_A\rangle_0\Bigg[\frac{\sin(k_0nd)}{k_0nd}+\frac{\cos(k_0nd)}{k_0^2n^2d^2}-\frac{\sin(k_0nd)}{k_0^3n^3d^3}\Bigg]\theta(ct-nd)+\langle\hat{\pi}_A^\dagger\hat{\pi}_B\rangle_0 2\times\Bigg\{\Bigg[-\frac{\cos(k_0R_n)}{k_0^2R_n^2}+\frac{\sin(k_0R_n)}{k_0^3R_n^3}\Bigg]+\frac{n^2d^2}{R_n^2}\times\Bigg[\frac{\sin(k_0R_n)}{k_0R_n}+3\frac{\cos(k_0R_n)}{k_0^2R_n^2}-3\frac{\sin(k_0R_n)}{k_0^3R_n^3}\Bigg]\times\theta(ct-R_n)\Bigg\}\Bigg)\Bigg). \tag{19}$$

We note in this case the absence of the long-range interaction term proportional to R^{-1} which corresponds to a less efficient head on dipole-dipole interaction. This is expressed by the numerical computation of Fig. 3(b), which shows the temporal behavior of the function which modulates the mutual terms,

$$D(t,R)=3\Bigg[-\frac{\cos(k_0R)}{k_0^2R^2}+\frac{\sin(k_0R)}{k_0^3R^3}\Bigg]\theta(ct-R)+3\times\sum_{n=1}^{+\infty}(-|r|)^n\Bigg\{2\Bigg[-\frac{\cos(k_0R_n)}{k_0^2R_n^2}+\frac{\sin(k_0R_n)}{k_0^3R_n^3}\Bigg]+\left(\frac{nd}{R_n}\right)^2\Bigg[\frac{\sin(k_0R_n)}{k_0R_n}+3\frac{\cos(k_0R_n)}{k_0^2R_n^2}-3\frac{\sin(k_0R_n)}{k_0^3R_n^3}\Bigg]\Bigg\}\theta(ct-R_n). \tag{20}$$

In Figs. 3(a) and 3(b) the oscillatory behavior due to the cavity effect is superimposed on the causal step-function behavior expected in free space.

The causal nature of the two-dipole interaction within a microcavity given by Eqs. (17) and (18) could be verified by us in a previous experiment performed at a single-photon level [13] by taking advantage of the femtosecond temporal resolution of the up-conversion nonlinear optical gate, as already discussed, [14].

III. SUPERRADIANCE EMISSION RATE AND SECOND-ORDER CORRELATION FUNCTION OF THE TWO-DIPOLE RADIATED FIELD

The rate of superradiant emission of the two-dipole system in a microcavity can be calculated by following Dicke's theory for a two-level atom [8]. Let us consider the case of two dipoles prepared in the tripet entangled state,

$$|A,B\rangle=\frac{1}{\sqrt{2}}(|\uparrow,\downarrow\rangle+|\downarrow,\uparrow\rangle), \tag{21}$$

with the corresponding expected values of the atomic operators

$$\langle\hat{\pi}_A^\dagger\hat{\pi}_A\rangle_0=\tfrac{1}{2},\quad\langle\hat{\pi}_A^\dagger\hat{\pi}_B\rangle_0=\tfrac{1}{2}. \tag{22}$$

The temporal evolution of the excited level of dipole *A* expressed in Eq. (16) becomes

$$\frac{d\langle \hat{\pi}_A^\dagger \hat{\pi}_A \rangle_t}{dt} = -\Gamma \Bigg\{ 1 + \frac{3\hat{\mu}_i \hat{\mu}_h}{2k_0^3} C_{ih}^R [\sin(k_0 R)] \theta(ct-R) + \frac{3\hat{\mu}_i \hat{\mu}_h}{k_0^3} \sum_{n=1}^{+\infty} (-|r|)^n \{ C_{ih}^{nd} [\sin(k_0 nd)] \times \theta(ct-nd) + C_{ih}^{R_n} [\sin(k_0 R_n)] \theta(ct-R_n) \} \Bigg\}. \tag{23}$$

In the relevant case of two dipoles oriented along the **X** axis ($\alpha=0$) we can obtain the superradiant SE rate expressed as a function of R,

$$\Gamma_{\sup}(R) = \Gamma \Bigg\{ 1 + \frac{3}{2k_0^3} \Bigg[\sin(k_0 R) \Bigg(-\frac{1}{R^3} + \frac{k_0^2}{R} \Bigg) + \cos(k_0 R) \frac{k_0}{R^2} \Bigg] \theta(ct-R) + \frac{3}{k_0^3} \times \sum_{n=1}^{+\infty} (-|r|)^n \Bigg[\sin(k_0 nd) \Bigg(-\frac{1}{(nd)^3} + \frac{k_0^2}{nd} \Bigg) + \cos(k_0 nd) \frac{k_0}{(nd)^2} \Bigg] \theta(ct-nd) + \Bigg[\sin(k_0 R_n) \times \Bigg(-\frac{1}{R_n^3} + \frac{k_0^2}{R_n} \Bigg) + \cos(k_0 R_n) \frac{k_0}{R_n^2} \Bigg] \theta(ct-R_n) \Bigg\}. \tag{24}$$

In the limit $t>x/c$, $\theta(ct-x)=1$ and the temporal dependence can be neglected.

Note that this expression has been obtained in the case of strong atom-field coupling, a condition which is not usually met in the planar microcavity [18]. This implies that the condition $\tau_c \gg 1/\Omega$, where τ_c and $1/\Omega$ represent the cavity photon lifetime and the period of Rabi oscillation, is not satisfied in our experiment. As a consequence, the superradiant time phenomenology accounted for in the present work only relates to the behavior of the diagonal elements of the density matrix of the active dipoles [19].

Figure 4 shows the behavior of $\Gamma_{\sup}(R)$, normalized to Γ, as a function of the normalized distance $\gamma = R/l_c$. The parameters adopted in the numerical analysis are those of our experiment, $f=3000$, $l_c = 77\,\mu$m. Furthermore, the order n of the series is truncated at a proper value $M=200$ and the contribution of the terms $n>M$ has been neglected. It is found that for maximum superradiance ($R \approx 0$) the value of $\Gamma(R)$ is *twice* as large as the value Γ_∞ of the case of two independent dipoles ($R \gg l_c$).

This property, which manifests itself as the characteristic signature of superradiance, has been verified in our experiment by the measurement performed with a standard Hanbury-Brown-Twiss (HBT) apparatus of the temporal evolution of the second-order correlation function (see configuration A of Fig. 5, Sec. IV). We introduce here its expression in order to get a better insight into the process: $F(\tau)$

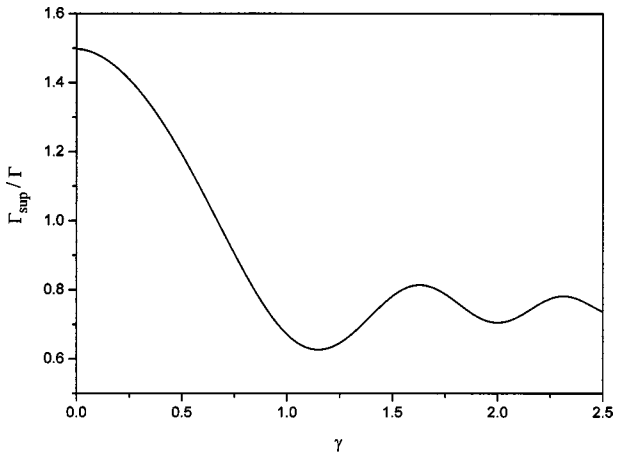

FIG. 4. Superradiant decay rate as a function of the interatomic distance γ of two parallel dipoles oriented along the **X** axis and located on the plane $\mathbf{Z}=\mathbf{0}$ of a symmetrical microcavity. Cavity finesse $f=3000$.

$\propto \langle \hat{\mathbf{E}}^-(t) \cdot \hat{\mathbf{E}}^-(t+\tau) \hat{\mathbf{E}}^+(t+\tau) \cdot \hat{\mathbf{E}}^+(t) \rangle$. Here τ corresponds to the time delay between two photodetections. Let us refer to the case of two dipoles parallel to the **X** axis ($\alpha=0$) (cf. Fig. 1). They are excited at the time $t_0=0$ and the emitted radiation is observed at a later time t by a detector located on the **Z** axis at a distance $Z \gg \lambda$ from the center of the cavity. In the Heisenberg representation, the field can be expressed in terms of the dipole transition operators $\hat{\pi}_A(t)$ and $\hat{\pi}_B(t)$ [2],

$$\hat{\mathbf{E}}^+(z,t) = -\Theta \sqrt{(1-|r|^2)} \sum_{n=0}^{\infty} r^{2n} \Bigg\{ \Bigg[\hat{\boldsymbol{\pi}}_A \Bigg(t - \frac{Z+2nd}{c} \Bigg) + \hat{\boldsymbol{\pi}}_B \Bigg(t - \frac{Z+2nd}{c} \Bigg) \Bigg] \frac{1}{Z+2nd} + r \Bigg[\hat{\boldsymbol{\pi}}_A \Bigg(t - \frac{Z+(2n+1)d}{c} \Bigg) + \hat{\boldsymbol{\pi}}_B \Bigg(t - \frac{Z+(2n+1)d}{c} \Bigg) \Bigg] \frac{1}{Z+(2n+1)d} \Bigg\}. \tag{25}$$

In the above equation the effect of multiple intracavity reflections has been considered, r represents the reflection coefficient of the mirrors at normal incidence, and Θ is a constant depending on the wavelength of emission and the dipoles orientation [2]. Since the radiative decay time of the dipoles is much longer than its period of oscillation we can ignore the differences between the retardation times in all the terms which contribute to the radiated field. As a consequence, the expressions of the electric field and of its Hermitian-conjugate become

$$\hat{\mathbf{E}}^+(Z,t) = -\Theta(1+r) \sqrt{1-|r|^2} \Bigg[\hat{\boldsymbol{\pi}}_A \Bigg(t - \frac{Z}{c} \Bigg) + \hat{\boldsymbol{\pi}}_B \Bigg(t - \frac{Z}{c} \Bigg) \Bigg] \sum_{n=0}^{\infty} r^{2n}, \tag{26}$$

$$\hat{\mathbf{E}}^{-}(Z,t) = -\Theta(1+r^{*})(\sqrt{1-|r|^{2}})^{*}\left[\hat{\boldsymbol{\pi}}_{A}^{\dagger}\left(t-\frac{Z}{c}\right) + \hat{\boldsymbol{\pi}}_{B}^{\dagger}\left(t-\frac{Z}{c}\right)\right]\sum_{n=0}^{\infty} r^{*2n}. \tag{27}$$

We can write the second-order correlation function of the field radiated by dipoles A and B as

$$F(\tau) = \langle[\hat{\mathbf{E}}_{A}^{-}(t)+\hat{\mathbf{E}}_{B}^{-}(t)]\cdot[\hat{\mathbf{E}}_{A}^{-}(t+\tau)+\hat{\mathbf{E}}_{B}^{-}(t+\tau)] \times[\hat{\mathbf{E}}_{A}^{+}(t+\tau)+\hat{\mathbf{E}}_{B}^{+}(t+\tau)]\cdot[\hat{\mathbf{E}}_{A}^{+}(t)+\hat{\mathbf{E}}_{B}^{+}(t)]\rangle. \tag{28}$$

By substituting the expressions of the electric-field operator given in Eqs. (24) and (25), we obtain

$$F(\tau) \propto \langle[\hat{\pi}_{A}^{\dagger}(t)+\hat{\pi}_{B}^{\dagger}(t)][\hat{\pi}_{A}^{\dagger}(t+\tau)+\hat{\pi}_{B}^{\dagger}(t+\tau)][\hat{\pi}_{A}(t+\tau) + \hat{\pi}_{B}(t+\tau)][\hat{\pi}_{A}(t)+\hat{\pi}_{B}(t)]\rangle. \tag{29}$$

Because of the operators commutation properties [19] the contribution due to different atoms vanishes and we obtain

$$F(\tau) \propto \sum_{i=A,B}\langle\hat{\pi}_{i}^{\dagger}(t)\hat{\pi}_{i}^{\dagger}(t+\tau)\hat{\pi}_{i}(t+\tau)\hat{\pi}_{i}(t)\rangle + \sum_{i\neq}\{\langle\hat{\pi}_{i}^{\dagger}(t)\hat{\pi}_{j}^{\dagger}(t+\tau)\hat{\pi}_{j}(t+\tau)\hat{\pi}_{i}(t)\rangle + \langle\hat{\pi}_{i}^{\dagger}(t)\hat{\pi}_{j}^{\dagger}(t+\tau)\hat{\pi}_{i}(t+\tau)\hat{\pi}_{j}(t)\rangle\}. \tag{30}$$

Moreover, by accounting for the antibunching character of the output radiation, we have

$$F(\tau) \propto \sum_{i\neq j}[\langle\hat{\pi}_{i}^{\dagger}(t)\hat{\pi}_{j}^{\dagger}(t+\tau)\hat{\pi}_{j}(t+\tau)\hat{\pi}_{i}(t)\rangle + \langle\hat{\pi}_{i}^{\dagger}(t) \times\hat{\pi}_{j}^{\dagger}(t+\tau)\hat{\pi}_{i}(t+\tau)\hat{\pi}_{j}(t)\rangle] \tag{31}$$

for $i, j = A,B$.

We make further use of the ansatz $\hat{\pi}(t) = \hat{\pi}(0) \times\exp\{-[i(2\pi c/\lambda)+(1/2)\Gamma(R)]t\}$, implying that no causal interdipole interaction is established at $t_0 = 0$ [6,7]. By averaging over all the possible times of emission of the first photon, we found by a simple integration

$$F(\tau) \propto \exp[-\Gamma(R)|\tau|], \tag{32}$$

with the explicit expression of $\Gamma(R)$, the function of the *free-space* SE rate Γ given in Eq. (23).

This result guarantees the possibility of measuring the enhancement of the superradiant spontaneous-emission rate of a two-dipole system trapped in a microcavity by a HBT experiment, as described in Sec. IV. Precisely, we have measured the *normalized* quantity $F(\tau) = \lim_{T\to\infty} g^{(2)}(\tau)[T^{-1}\int_{0}^{T} g^{(2)}(\tau)d\tau]^{-1}$, where $g^{(2)}(\tau)$ corresponds to the degree of second-order temporal coherence of the radiation emitted by the microcavity. By referring to configuration A of Fig. 5 and assuming the exponential decay for the SE probability, $F(\tau)$ may be also interpreted as the normalized time probability distribution of detecting $n_{\mathbf{k}} = 2$ photons emitted over the output mode $\mathbf{k}$ and $n_{\mathbf{k}'} = 0$ photons over the mode $\mathbf{k}'$, symmetric to $\mathbf{k}$. Because of its normalization properties $F(\tau)$ is proportional at time $\tau = 0$ to the probability of *simultaneous emission* of two photons over the output mode $\mathbf{k}$ and zero photons over $\mathbf{k}'$, $F(0) = AP(2,0)$. A similar argument can be applied when $F(\tau)$ is determined by configuration B of Fig. 5. In this case we get the probability of simultaneous emission of one photon over the output mode $\mathbf{k}$ and one photon over $\mathbf{k}'$: $F(0) = AP(1,1)$.

IV. EXPERIMENTAL RESULTS

The microcavity adopted in the experiment consisted of a single-longitudinal mode Fabry-Perot interferometer, terminated by two parallel, plane multilayer dielectric mirrors, highly reflecting ($\mathcal{R} \equiv |r|^2 = 0.999$) at the resonant wavelength of emission ($\lambda = 700$ nm) and highly transparent at the excitation wavelength $\lambda_p < \lambda$. The cavity ''finesse'' was $f = 3000$. This value determines the time of establishment of the e.m. mode within the microcavity storage time, corresponding to the ''coherence time'' of the emitted particles: $\tau_c \approx 1$ ps [18,20]. The active medium was given by a 10^{-5} mole/liter concentration of Oxazine 725 dye molecules dispersed in a polymethyl methacrylate (PMMA) solid film. The experiment was carried out either at room temperature or at the liquid-nitrogen temperature (LNT). A longer fluorescence decay time was measured in the second case because of the increased quantum yield of the dye molecules [21].

Molecular excitation was performed by an amplified colliding pulse mode-locking (CPM) dye laser, operating at $\lambda_p = 615$ nm. Two identical excitation pulses, with duration $\delta t = 80$ fs, were focused by means of a 20 cm $f/1$ lens within the microcavity in two spots with diameter $\varphi = 10\,\mu$m at an externally adjustable mutual transverse distance R along the $\mathbf{Y}$ axis by a fine adjustment of the angle between the two excitation beams. Temporal delay Δt between the two excitation pulses was varied by means of a step by step translation stage with spatial resolution of 1 μm.

The photons emitted over the forward mode of the microcavity were detected by cooled, avalanche single photon-counting modules EGG-SPCM200, indicated by D_1, D_2, D_3 in Fig. 5, with a typical quantum efficiency of 65%. The number of molecules in each spot was $\approx 10^5$ but, because of the limited values of their quantum yield and of the coupling efficiency of the cavity over the forward mode ($\approx$2%) [22], only few active molecules could radiate in the direction perpendicular to the mirrors. A careful adjustment of the pump energy could bring to the peculiar condition of *single-photon* emission from the microcavity following any single-laser pulse excitation. This condition could be tested experimentally by use of suitable Hanbury-Brown-Twiss (HBT) interferometric configurations involving each or, alternatively, both output modes, $\mathbf{k}$ and $\mathbf{k}'$, corresponding to the configurations A and B of Fig. 5 [5,19]. The HBT coincidence rate, evaluated as the ratio between the number of spurious two-detector coincidences and the number of detected ''singles''

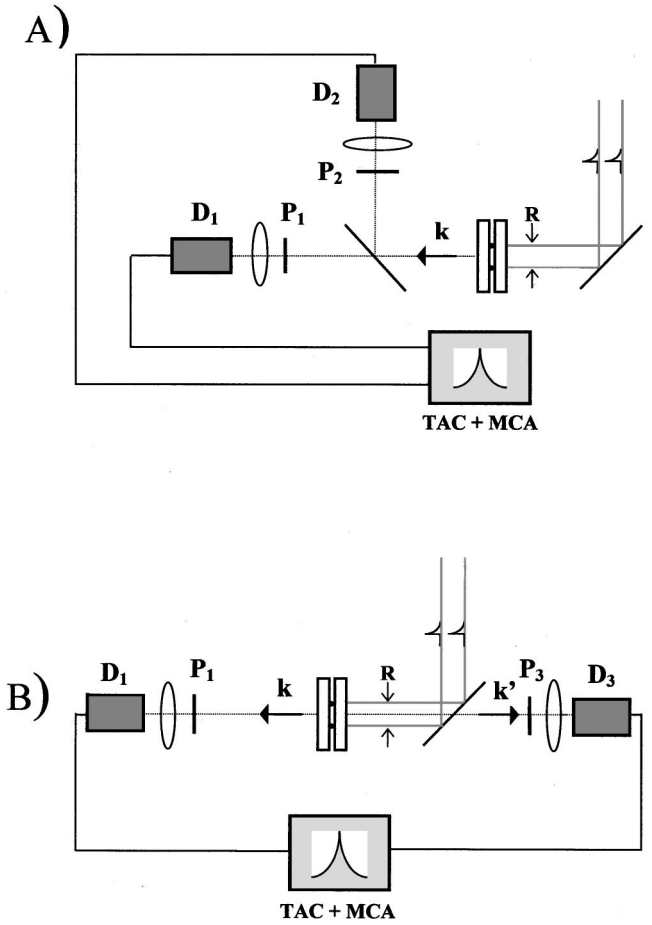

FIG. 5. Optical configurations *A* and *B* of the Hanbury-Brown-Twiss interferometers adopted in the experiment.

per second, was found less than 10^{-3}. The HBT measurements showed a striking evidence of the highly nonclassical, photon *antibunching* process, i.e., implying a very small value of the field's degree of second-order coherence: $g^{(2)} \ll 1$. As an example, a typical value of the second-order coherence degree, $g^{(2)}=4,\ 3\times10^{-2}$ was determined with configuration A on the basis of the following results: the number of detected coincidences is 3, the detected "singles" at the output of detectors $D_1=3810$ and $D_2=3250$, and the dimension of the statistical sample is 1.8×10^5 laser pulse excitation events. The evaluation of $g^{(2)}$ was carried out by detecting the photons within time windows of 5 ns following each excitation laser pulse and by means of a photon-counter Stanford Research SR 400.

As far as the time correlation measurements are concerned, these were carried out by feeding a time-to-amplitude converter (TAC) with the standard TTL output pulses of couples of detectors. The TAC (Silena 7412), which allowed us to monitor the time interval between the pulses of different detectors with a resolution of 50 ps, was connected to a multichannel analyzer (MCA) (Silena 7923-2048). The dye emission radiation, spectrally filtered by the microcavity, was spatially selected over the forward mode by aligning the two detectors (with active diameters of nearly 100 μm) in the focal plane of two 5 cm $f/1$ lenses. The residual stray light was removed by inserting two interference filters centered at $\lambda=700$ nm before the detectors.

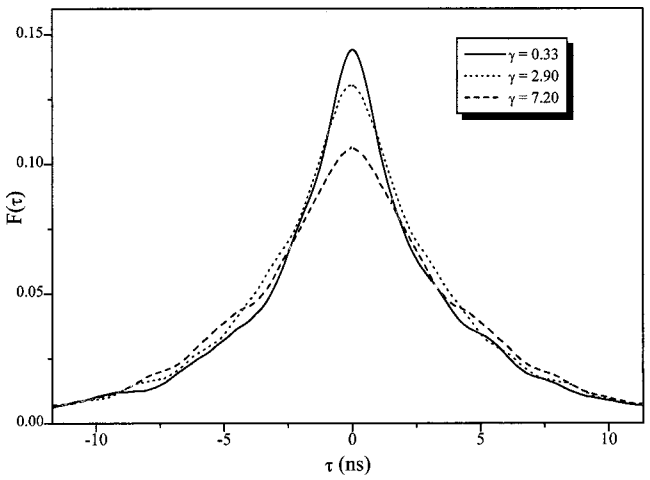

FIG. 6. Experimental normalized MCA distributions obtained at LNT for $\gamma=0.33$, $\gamma=2.9$, and $\gamma=7.2$. Dipoles oriented along the **X** axis.

Because of the random orientation of the active molecules the output radiation was found slightly (20%) linearly polarized along the (linear) polarization of the excitation laser beams [22]. In order to investigate the emission properties of the active dipoles along the orthogonal transverse spatial directions **X** and **Y**, the output radiation detected by each D_j was filtered by adjustable optical polarization analyzers P_j. The polarization of the excitation pulses was set oriented along **X**.

Two different experimental configurations, involving two laser-pulse excitations, were investigated. Configuration A in Fig. 5: by adoption of D_1 and D_2 as *start* and *stop* devices for the TAC, we could measure the joint probability of photon pairs emission over the single output mode **k**, i.e., on one side of the microcavity. Configuration B: the adoption of D_1 and D_3 as *start-stop* devices, allowed direct HBT investigations on both output modes **k** and **k**′ of the microcavity, here used as a kind of *active beam splitter* [5].

Typical experimental results corresponding to the temporal evolution of the coincidence probability, obtained at LNT in the case of two dipoles oriented along the **X** axis, are shown in Fig. 6 for three values of the mutual distance, $\gamma=R/l_c=0.33$, 2.9, and 7.2, being $l_c=77\ \mu$m for our experiment. A relevant variation of the coincidence probability is observed at $\tau=0$ for R varying from the case of fully independent dipoles to that of two dipoles interacting within the same spatial mode. Figure 7 allows us to compare, on a semilogarithmic plot, the corresponding temporal decay traces of $F(\tau)$. The decay rate is enhanced of a factor 1.8 for $R\rightarrow0$. Note that the decay rate of $F(\tau)$ measured at the largest distance is nearly equal to the single molecule spontaneous-emission rate in a microcavity [2].

The experimental results reported in Figs. 8(a)–8(c) allow us to compare the process of two-dipole interaction for different orientations of the emitting dipoles. In spite of the shorter decay times due to the fact that the measurements have been performed at room temperature, we can compare

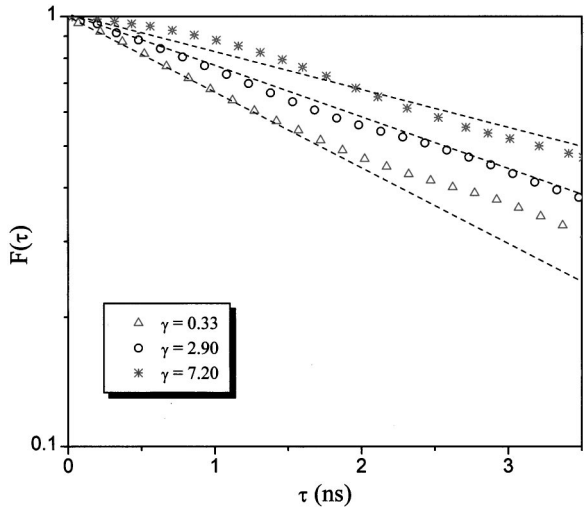

FIG. 7. Semilogarithmic plot of the two-photon MCA distributions $F(\tau)$ of Fig. 6, near $\tau=0$. The dashed straight lines represent the corresponding time decays evaluated by following the expression of $\Gamma(R)$ reported in Eq. (22).

the results obtained for the interdipole distances $R=30$ and 600 μm. We observe that the enhancement effect vanishes for two mutually orthogonal dipoles while it is sensibly reduced in the case of two dipoles oriented along the **Y** axis, corresponding to the less efficient head-on dipole-dipole interaction.

The above results demonstrate that the peculiar geometry of the microcavity is instrumental in the determination of the *time* behavior of a quantum SE decay process within an interatomic interaction. This *mesoscopic* character of the device is precisely ascribable to the fact that the wavelength λ of the confined photon is of the order of the relevant dimension d of the confining device. This is a common characteristics of all nanostructures that exhibit quantum properties. In this perspective, it is expected that also the *spatial* behavior of some relevant dynamical process should be affected by the peculiar quantum properties of the device.

In the new experiment, the planar symmetric microcavity has been adopted to investigate the spatial statistical distribution of the couples of photons emitted over the two allowed microcavity output modes **k** and **k**′ under corresponding couples of excitation laser pulses. This process has been investigated with the same microcavity by both experimental configurations A and B, Fig. 5, and for very small time delay $\tau\approx 0$. Precisely, we have measured the probability $P(2,0)$ of the simultaneous photodetections realized by D_1 and D_2 coupled to the external output mode **k**, and the probability $P(1,1)$ of the simultaneous photodetections realized by D_1 and D_3 coupled to the counterpropagating external output modes **k** and **k**′. According to a ''classical'' Maxwell-Boltzmann partition statistics, and by accounting for the couples of detection events, we expect $P(1,1)=2P(2,0)$.

In Fig. 9 we report the results of this experiment. Here the values of the probability are referred to the total number of two-photon detection events actually registered in the experiment. Furthermore, by reporting the experimental data obtained by configuration A, we have taken care of the effect of

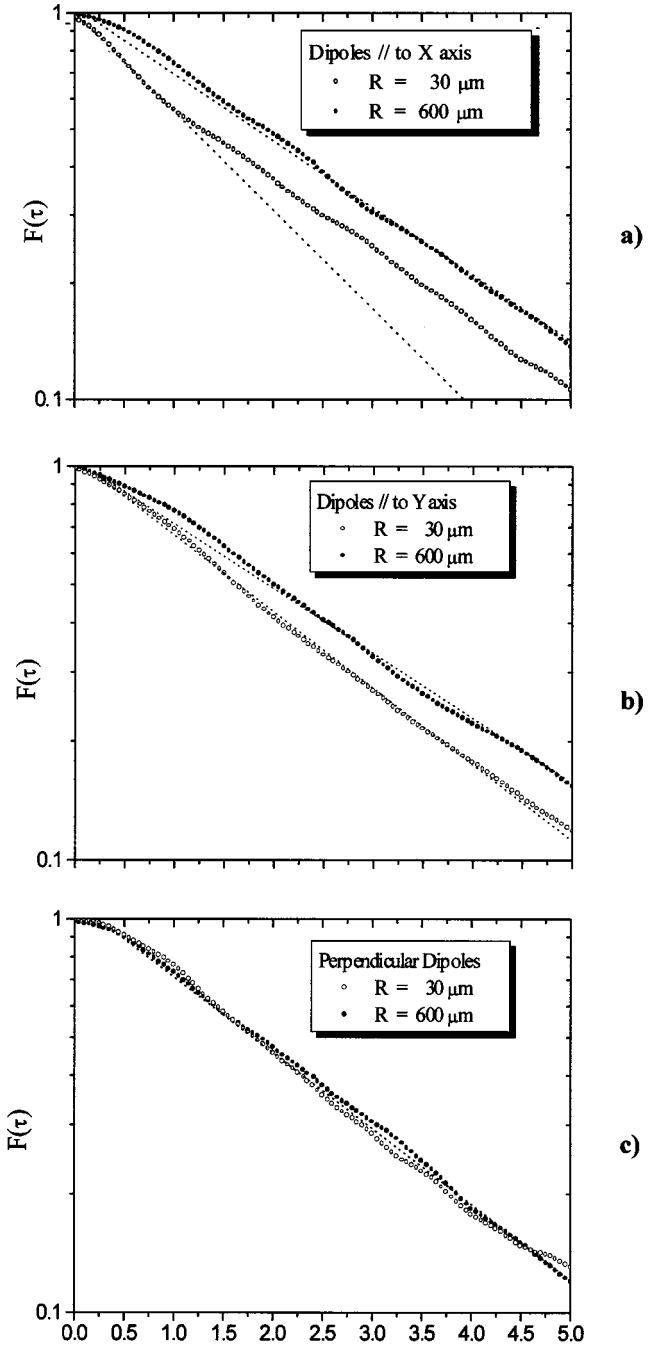

FIG. 8. Semilogarithmic plot of $F(\tau)$ at room temperature, corresponding to $R=30$ and 600 μm for the three cases: (a) dipoles parallel to the **X** axis, (b) dipoles parallel to the **Y** axis, and (c) perpendicular dipoles. The dashed straight lines shown in each plot correspond to the best fits of the experimental curves.

the symmetrical beam splitter placed at the output of the microcavity. The experimental results show that the classical condition $P(1,1)=2P(2,0)$ is verified indeed for a large interdipole distance: $R\gg l_c$. However, for shorter distances $R\lesssim l_c$, the relative values of the probabilities converge toward the common value: $P(1,1)=P(2,0)$. This implies that a quantum Bose-Einstein partition process determines the photoemission over the external modes of the microcavity. The unambiguous conclusion is that, for $R/l_c\ll 1$, the two pho-

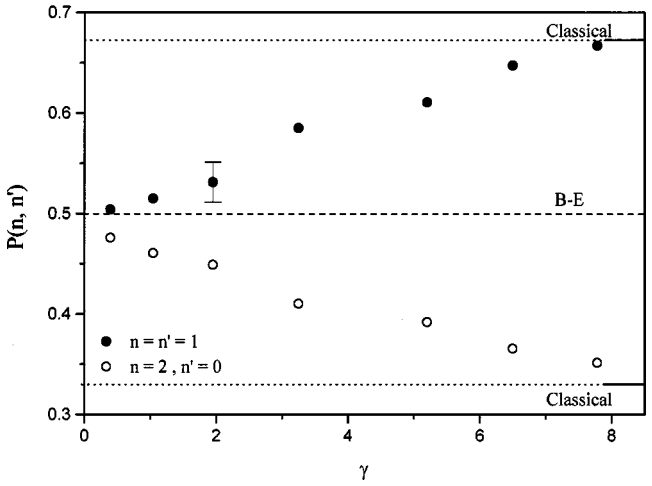

FIG. 9. Two-photon partition probabilities $P(1,1)$ and $P(2,0)$ over the two output channels $\mathbf{k}$, $\mathbf{k}'$ and detected at $\tau \approx 0$ as function of the relative transverse interdipole distance $\gamma = R/l_c$.

tons tend to be emitted both at the *same time* and over the *same spatial* mode of the microcavity.

V. ANALYSIS OF THE RESULTS AND DISCUSSION

The realization of a quantum statistical photon distribution law over the two output sides of an optical cavity is unexpected in the usual laser dynamics and has never been investigated so far. We may explain this remarkable phenomenon by expressing the density operator which represents the state of the field for the two relevant cases, $R \ll l_c$ and $R \gg l_c$.

Let us consider first the condition $R \ll l_c$. In this case, the two photons are emitted over the common spatial mode of the microcavity (cf. Fig. 5). It is given by the linear superposition of the modes with the *internal* momenta $\mathbf{p} = \hbar \mathbf{k}$, $\mathbf{p}' = \hbar \mathbf{k}' = -\mathbf{p}$, directed towards the *left* (l) and *right* (r) sides of the cavity. In this condition, the appropriate expression of the density operator is

$$\rho_1 = \pi^{-2} \int \int d\varphi \, d\varphi' \cos^2 \varphi \cos^2 \varphi' (\hat{a}_l^\dagger + e^{i\varphi} \hat{a}_r^\dagger)(\hat{a}_l^\dagger + e^{i\varphi'} \hat{a}_r^\dagger) |\mathrm{vac}\rangle\langle \mathrm{vac}| (\hat{a}_l + e^{-\varphi'} \hat{a}_r)(\hat{a}_l + e^{-i\varphi} \hat{a}_r), \tag{33}$$

where the vacuum field is represented by $|\mathrm{vac}\rangle \equiv |0,0\rangle \equiv |l = 0, r = 0\rangle$.

In the above equation we have taken into account the enhancement of spontaneous-emission probability in the plane microcavity as function of Z by means of the distribution function $\pi^{-1} \cos^2 \varphi$ [2]. Moreover, because of the uniform molecules distribution between the two mirrors, the phases $\varphi = \pi Z/d$, $\varphi' = \pi Z'/d$ account for the random position, shot to shot, of the emitting dipoles along the longitudinal coordinate Z. By performing integration and normalization we obtain

$$\rho_1 = \tfrac{1}{3}(|2,0\rangle\langle 2,0| + |1,1\rangle\langle 1,1| + |0,2\rangle\langle 0,2|), \tag{34}$$

with, e.g., $|2,0\rangle \equiv |l = 2, r = 0\rangle$ or, generally, $|x,y\rangle \equiv |n_{\mathbf{k}}\rangle \otimes |n_{\mathbf{k}'}\rangle$.

Suppose now that the transverse distance between the emitting dipoles is large, $R \gg l_c$. In this case the two photons are emitted over two *distinct* spatial modes, which are given by the superposition of two couples of distinct traveling-wave modes l, l' and r, r' directed towards the left and the right sides of the cavity. In this case the field of the system is given by the expression

$$\rho_2 = \pi^{-2} \int \int d\varphi \, d\varphi' \cos^2 \varphi \cos^2 \varphi' (\hat{a}_l^\dagger + e^{i\varphi} \hat{a}_r^\dagger)(\hat{a}'^\dagger_l + e^{i\varphi'} \hat{a}'^\dagger_r) |\mathrm{vac}\rangle\langle \mathrm{vac}| (\hat{a}'_l + e^{-i\varphi'} \hat{a}'_r)(\hat{a}_l + e^{-i\varphi} \hat{a}_r), \tag{35}$$

where the operators $\hat{a}_l$, $\hat{a}'_l$, $\hat{a}_r$, $\hat{a}'_r$ correspond to the modes l, l', r, r' and the vacuum field is represented as $|\mathrm{vac}\rangle \equiv |0,0;0,0\rangle \equiv |l = 0,\ l' = 0;\ r = 0,\ r' = 0\rangle$. It is found in this case

$$\rho_2 = \tfrac{1}{4}(|1,1;0,0\rangle\langle 1,1;0,0| + |1,0;0,1\rangle\langle 1,0;0,1| + |0,1;1,0\rangle \times \langle 0,1;1,0| + |0,0;1,1\rangle\langle 0,0;1,1|). \tag{36}$$

The photons emerging from the left or right sides of the cavity are finally focused outside the cavity over the photocathodes of the detectors D_1, D_2, D_3, having selected the polarization according to the experimental procedure described in above and in Sec. IV.

By this theory we are able to justify the experimental results. In the case of a *single* spatial mode, $R \ll l_c$, the probabilities of detecting couples of particles either on the left or on the right of the cavity: $P(2,0) = \langle 2,0|\rho_1|2,0\rangle = \frac{1}{3}$, $P(0,2) = \langle 0,2|\rho_1|0,2\rangle = \frac{1}{3}$ are equal to the probability of detecting one photon in each side: $P(1,1) = \langle 1,1|\rho_1|1,1\rangle = \frac{1}{3}$.

The last result corresponds exactly to the quantum Bose-Einstein (BE) statistics. According to this theory the probability of distributing N indistinguishable particles among G "boxes" is independent of the set of occupancies of the boxes, here indicated in short by $\{n_i\}$, and it is given by: $P\{n_i\} = [(G-1)!N!/(G+N-1)!]$ [23].

In the case of a large distance between the active dipoles, $R \gg l_c$, the two photons are emitted over two distinct spatial modes and have to be considered distinguishable. In this case the partition probabilities are $P(2,0) = \langle 1,1;0,0|\rho_2|1,1;0,0\rangle = \frac{1}{4}$, $P(0,2) = \langle 0,0;1,1|\rho_2|0,0;1,1\rangle = \frac{1}{4}$ $P(1,1) = \langle 0,1;1,0|\rho_2|0,1;1,0\rangle + \langle 1,0;0,1|\rho_2|1,0;0,1\rangle = \frac{1}{2}$, which is exactly the classical result expected in the case of the binomial partition statistics: $P\{n_i\} = G^{-N} N!/(n_l! n_r!)$. Here, the boxes labeled by $i = l$ and $i = r$ express detection on either side of the cavity, as said. Note that the two statistical formulas just given reproduce the results of the experiment for $G = 2$, $n_l + n_r = N = 2$.

As a conclusion, two (or more) photons become indistinguishable and follow the quantum BE statistics when they are emitted over the common space-time mode of the microcavity. The same effect could also be detected by exciting a large unknown number of active molecules in the microcav-

ity. In this case the quantum character of the multiphoton statistical process could be identified by the experimental determination of the two-channel ''quantum noise function,'' previously introduced in a different context [24].

As a final comment, we could say that the physical condition of two interacting dipoles within a microcavity identifies *exactly* the growing point of the ''thresholdless microlaser'' [3], in such a way that the superradiance is responsible, at a fundamental microscopic level, of the very first stages of the collective dynamics of this process. All this may have important consequences because of modern technological implications on the knowledge of the behavior of the vertical cavity surface-emitting laser (VCSEL) [25].

VI. CONCLUSIONS

In this paper we have discussed the realization of the process of two-dipole Dicke superradiance in a planar optical microcavity. The main theoretical results of the paper are Eqs. (17) and (19), calculated in the Heisenberg representation, for the temporal evolution of the excited dipole *A* interacting with dipole *B* within the microcavity. The two expressions corresponds to the different spatial orientations (dipoles parallel to the **X** and to the **Y** axes, respectively) of the parallel dipoles. The superradiant SE rate in the relevant case of two dipoles oriented along the **X** axis is given in Eq. (24). Then an experiment is presented aimed at the verification of the relevant theoretical results by the investigation of the spontaneous emission of two molecules trapped in a polymer matrix within a single-mode optical microcavity. The investigation of superradiance in the space domain has allowed us to discover the transition from the classical to the quantum partition statistics of the photons emitted over the two output modes of the microcavity for decreasing of the interdipole distance *R*.

ACKNOWLEDGMENT

This research was carried out under CEE-TMR Contract No. ERBFMRXCT96-0066.

[1] W. Jhe, A. Anderson, E. A. Hinds, D. Meschede, L. Moi, S. Haroche, Phys. Rev. Lett. **58**, 666 (1987); F. De Martini, G. Innocenti, G. R. Jacobovitz, and P. Mataloni, *ibid.* **59**, 2955 (1987).
[2] F. De Martini, M. Marrocco, P. Mataloni, L. Crescentini, and R. Loudon, Phys. Rev. A **43**, 2480 (1991).
[3] F. De Martini and G. R. Jacobovitz, Phys. Rev. Lett. **60**, 1711 (1988); F. De Martini, F. Cairo, P. Mataloni, and F. Verzegnassi, Phys. Rev. A **46**, 4220 (1992).
[4] F. De Martini, M. Marrocco, and D. Murra, Phys. Rev. Lett. **65**, 1853 (1991).
[5] F. De Martini, G. Di Giuseppe, and M. Marrocco, Phys. Rev. Lett. **76**, 900 (1996); F. De Martini, O. Jedrkiewicz, and P. Mataloni, J. Mod. Opt. **44**, 2053 (1997).
[6] F. De Martini and M. Giangrasso, Appl. Phys. B: Lasers Opt. **60**, S-49 (1995).
[7] F. De Martini and M. Giangrasso, in *Amazing Light*, edited by R. Y. Chiao (Springer, New York, 1996), p. 197.
[8] R. B. Dicke, Phys. Rev. **93**, 99 (1954).
[9] M. Gross and S. Haroche, Phys. Rep. **93**, 301 (1982).
[10] R. G. De Voe and R. G. Brewer, Phys. Rev. Lett. **76**, 2049 (1996).
[11] A. Aiello, F. De Martini, M. Marrocco, and P. Mataloni, Opt. Lett. **20**, 1492 (1995).
[12] K. Ujihara, Jpn. J. Appl. Phys., Part 2 **30**, L901 (1991).
[13] F. De Martini, O. Jedrkiewicz, and P. Mataloni, J. Nonlinear Opt. Phys. Mater. **7**, 121 (1998).
[14] P. Mataloni, O. Jedrkiewicz, and F. De Martini, Phys. Lett. A **243**, 270 (1998).
[15] P. Mataloni, E. De Angelis, and F. De Martini, Phys. Rev. Lett. **85**, 1420 (2000).
[16] M. Ley and R. Loudon, J. Mod. Opt. **34**, 227 (1987).
[17] A. Takada and K. Ujihara, Opt. Commun. **160**, 146 (1999).
[18] E. A. Hinds, in *Advances in AMO Physics*, edited by P. R. Berman (Academic, New York, 1994); O. Jedrkiewicz and R. Loudon, Phys. Rev. A **60**, 4951 (1999).
[19] R. Loudon, *The Quantum Theory of Light* (Oxford University Press, New York, 2000).
[20] P. Mataloni, A. Aiello, D. Murra, and F. De Martini, Appl. Phys. Lett. **65**, 1891 (1994).
[21] O. Svelto, *Principles of Lasers* (Plenum, New York, 1989), Chap. 2.
[22] S. Ciancaleoni, P. Mataloni, O. Jedrkiewicz, and F. De Martini, J. Opt. Soc. Am. B **14**, 1556 (1997).
[23] L. Landau and E. Lifshitz, *Statistical Physics* (Pergamon, London, 1958), Chap. 5; F. Mandl, *Statistical Physics* (Wiley, New York, 1988), Chap. 11; J. Tersoff and D. Bayer, Phys. Rev. Lett. **50**, 553 (1983).
[24] F. De Martini and S. Di Fonzo, Europhys. Lett. **10**, 123 (1989).
[25] Y. Yamamoto and R. E. Slusher, Phys. Today **46** (6), 66 (1993).